Jonas Massmann*, Timo Tigges, and Reinhold Orglmeister

Continuous signal quality estimation for robust heart rate extraction from photoplethysmographic signals

https://doi.org/10.1515/cdbme-2020-3131

Abstract: This study presents a novel method for estimating the signal quality of photoplethysmographic (PPG) signals. For this purpose a robust classifier is implemented and evaluated by using finger- and inear-PPG. A new procedure is proposed, which uses feature reduction to determine the Mahalanobis distance of the PPG-pulses to a statistical reference model and thus facilitates a robust heart rate extraction. The evaluation of the algorithm is based on a classical binary classification using a manually annotated gold standard. For the finger-PPG a sensitivity of 86 ± 15 % and a specificity of 94 ± 13 % was achieved. Additionally, a novel classification method which is based on a continuous signal quality index is used. Pulse rate estimation errors greater than 5 BPM can be detected with a sensitivity of 91 ± 13 % and a specificity of 91 ± 15 %. Also, a functional correlation between the signal quality index and the standard deviation of the pulse rate error is shown. The proposed classifier can be used for improving the heart rate extration in pulse rate variability analysis or in the area of mobile monitoring for battery saving.

Keywords: signal quality index, artifacts, pulse oximetry, photoplethysmography, heart rate

1 Introduction

Pulse oximetry is an inexpensive, optical measuring method, which has already become established as a standard procedure for non-invasive measurement of arterial oxygen saturation in 1987 [5]. Besides, other vital parameters such as blood pressure, pulse rate or respiration rate can be continuously determined with photoplethysmography (PPG). With its portable and cost-effective application, pulse oximetry is an important component in monitoring of critically ill patients. Also, the general interest in portable monitoring systems for the vital parameters has been rising for several years [1]. Due to the mobile application, however, it is highly susceptible to motion artifacts that make the signal unusable.

Therefore, an important aspect is the detection and interpretation of interferences in the signal. In the literature, numerous publications have appeared in recent decades on the detection of artifacts, which already detect disturbances with adequate accuracy. Nevertheless, motion artifacts in the PPG are still a major challenge and no gold standard for detection has yet been established.

It is noticeable that nearly all the analyzed publications are based on a hand-annotated gold standard. There is no uniform annotation of the pulses and the assessment of the signal quality is very individual. It is not clearly defined when the quality of the measurement is no longer sufficient and the pulse is not suitable for further analysis. For example, in [1] two independent annotators for the quality assessment of pulse waves could only achieve an average agreement of 66.04 % of all observations (kappa coefficient of $\kappa = 0.48$).

In this paper the following three questions are analyzed and discussed:

– How can motion artifacts in the PPG be better detected using a beat-to-beat algorithm?
– Which morphological features are suitable as a continuous signal quality index (SQI) for the quality assessment of pulse waves?
– Can morphological features be used to determine a certainty for an estimated pulse rate?

2 Methods

2.1 Algorithm

To estimate the pulse wave quality a robust classifier is implemented and evaluated. A new procedure is proposed, which uses feature reduction to determine the Mahalanobis distance (MD) of the PPG-pulses to a statistical reference model.

Prior to the actual pulse analysis, the raw signal $y_{raw}(n)$ is preprocessed and the individual pulses must be segmented. In the preprocessing a 4th order Butterworth lowpass filter with a cut-off frequency of 20 Hz and second filter stage

***Corresponding author: Jonas Massmann,** Chair of Electronics and Medical Signal Processing, Faculty of Electrical Engineering, Technical University Berlin, Einsteinufer 17, Berlin, Germany, e-mail: jonas.s.massmann@campus.berlin-tu.de
Timo Tigges, Reinhold Orglmeister, Chair of Electronics and Medical Signal Processing, Technische Universitat Berlin, Berlin, Germany

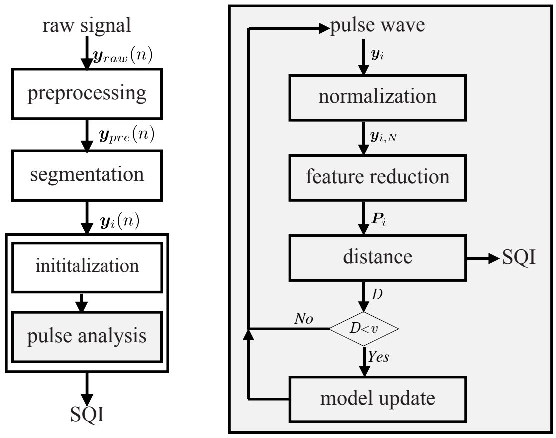

Fig. 1: Superordinate signal path. The schematic procedure of the beat-to-beat pulse analysis is highlighted in grey.

with a 4th order Butterworth high pass filter and a cut-off frequency of 0.5 Hz is used. To adjust the sampling frequencies of the PPG to the ECG, a spline interpolation is used, which is aligned with the sampling points of the ECG signal. The algorithm presented by Zong et. al. was used to detect the diastoles in finger- and inear-PPG [9], which were used for the pulse segmentation. After an initialization phase, quality estimation is performed beat-to-beat for each separated pulse. The signal flow is shown in figure 1 on the left side.

In pulse analysis, each pulse is normalized, modeled and evaluated separately. This beat-to-beat pulse analysis is shown in the flowchart in figure 1 on the right side. For normalization, the DC signal component is removed, by setting the value of the first diastole to zero. Since start and end value are not necessarily the same, a linear correction is applied. Furthermore, the pulse waves are normalized to the systolic point and thus have a uniform height of one. Finally, the length of each pulse is normalized, using the method for compression of ECG signals by Wei et al. [2], which is also suitable for PPG-signals [4]. A fixed length of 512 samples showed the best results.

In the feature reduction, each normalized pulse is reduced to a set of parameters $\boldsymbol{P}_i$, which are representing the signal morphology as accurately as possible. In the present study, three different types of signal modeling techniques are tested. The first analysed model is based on various morphological parameters. The second tested model is based on the system response, and the last model is using a curve-fitting procedure to remodel the pulse wave. All modeling functions are returning the vector $\boldsymbol{P}_i$, which is used for determining the quality index.

In the multivariate distribution $\boldsymbol{M}$ the parameter values $\boldsymbol{P}_i$ of N artifact-free pulses are stored. This constitutes the fundamental truth with which further pulses are rated. The fundamental statistical reference is formed during the initialization phase and updated during the further process. For the validation of the pulse quality, the distance D between the parameter vector $\boldsymbol{P}_i$ and the reference distribution $\boldsymbol{M}$ is calculated with $D = ||\boldsymbol{M} - \boldsymbol{P}_i||$. This can be solved using the MD with

$$D(\boldsymbol{P}_i, \boldsymbol{\mu}_{\boldsymbol{M},i}, \boldsymbol{\Sigma}_{\boldsymbol{M},i}) = \sqrt{(\boldsymbol{P}_{\boldsymbol{i}} - \boldsymbol{\mu}_{\boldsymbol{M}})^T\, \boldsymbol{\Sigma}_{\boldsymbol{M}}^{-1}\, (\boldsymbol{P}_i - \boldsymbol{\mu}_{\boldsymbol{M}})}, \tag{1}$$

whereby $\boldsymbol{\mu}_{\boldsymbol{M},i}$ is the empirical mean and $\boldsymbol{\Sigma}_{\boldsymbol{M},i}$ is the covariance matrix of $\boldsymbol{M}$ during analysis of the i-th pulse wave. The MD has the major advantage that it is scale-invariant, unitless and takes the correlation of the parameters into account.

To achieve an adaptive classification which can adapt to signal changes and is patient independent, artifact-free pulse waves are learned during the process. If the MD of a new pulse is less than or equal to a learning threshold $D \leq v$, its parameter vector $\boldsymbol{P}_i$ is added to the basic statistical truth $\boldsymbol{M}$. Due to performance reasons only the updated mean value and the covariance matrix is saved. Apart from the initialization phase, these can be calculated iteratively, which makes real-time implementation easier. Based on an initialization value, the i-th arithmetic mean value can be calculated elementwise with

$$\boldsymbol{\mu}_{\boldsymbol{M},i}(k) = \boldsymbol{\mu}_{\boldsymbol{M},i-1}(k)\frac{\boldsymbol{P}_i(k) - \boldsymbol{\mu}_{\boldsymbol{M},i-1}(k)}{N}[8]. \tag{2}$$

The iterative estimation of the covariance matrix results in

$$\boldsymbol{\Sigma}_M = \frac{1}{N-1}\sum_{n=1}^{N}(\boldsymbol{P}_i - \boldsymbol{\mu}_{\boldsymbol{M}})(\boldsymbol{P}_i - \boldsymbol{\mu}_{\boldsymbol{M}})^T[3]. \tag{3}$$

The MD results in the SQI. To achieve a bounded measure, the calculated distances D are considered in the space of the cumulated χ^2-distribution function F_χ given by

$$\text{SQI} = 100 \cdot \left(1 - F_\chi(D(\boldsymbol{P}_i, \boldsymbol{\mu}_{\boldsymbol{M},i}, \boldsymbol{\Sigma}_{\boldsymbol{M},i}) \mid M)\right). \tag{4}$$

$1 - F_\chi$ indicates the complement of the cumulative χ^2 distribution function. The degree of freedom is given by the number of modeling parameters M, according to the feature vector $\boldsymbol{P}_i$ length. Consequently, the SQI ranges over a limited range of values between 0 and 1, which simplifies later interpretation.

2.2 Data foundation

The data of a transmissive finger- and a reflective inear-PPG measurement of 30 healthy patients are used, resulting in an analysis of 160175 pulse waves. Due to the slightly different morphological properties, the finger- and inear-PPG signal are evaluated separately to see where the algorithm performs best. For validation, an additional ECG-signal was used, which was recorded simultaneously. The ECG was recorded with a sampling frequency of 500 Hz, whereas the PPG signals with a sampling frequency of 250 Hz. For further information about the data acquisition please refer to [7, 6].

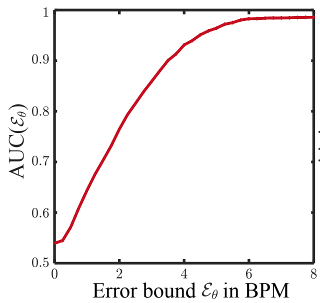

Fig. 2: Exemplary representation of AUC through a set of error bounds $\mathcal{E}_\theta$.

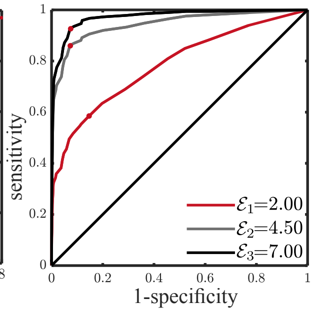

Fig. 3: Exemplary extract of ROC-curves over different pulse rate error bounds $\mathcal{E}_\theta$. The red dots mark the optimal Youden index.

2.3 Evaluation methods

The evaluation of the algorithm is conducted in three steps. First of all, a binary classification for the identification of strong artifacts in the PPG is conducted, which is evaluated using a manually annotated gold standard. The binary classification is rated by sensitivity and specificity. The optimization is based on the receiver operating characteristic curve and the area under the curve is used to determine the optimal threshold. In the first place, the different models are analyzed separately and the optimal model parameters are determined. Secondly, the optimal threshold for each model is searched by using the Youden index. With having the optimal threshold for each model, a comparison of the three models is done in the last step. This evaluation is performed separately for the finger-PPG and the inear-PPG.

In the second step of the evaluation the classification is based on a continuous signal quality index and is optimized and evaluated with respect to the estimation error of the pulse rate. The classification problem is reduced to a binary problem, using a variable error bound. Therefore, a ROC-analysis is done with multiple error bounds $\mathcal{E}_\theta$, shown in figure 3. This leads to a set of Area Under Curve (AUC) values (see figure 2), which can be summed up to a performance value and used as an optimization parameter. The actual optimization process is equivalent to the binary classification with a manually annotated gold standard, comprising a parameter finding of each model with an AUC optimization, a threshold optimization for every single model and a model comparison.

Finally, the classification is evaluated using a continuous SQI. For this purpose, the MD is considered as quantiles in the space of the χ^2-distribution function. It is assumed that the previously determined model of binary classification with a variable error bound is also best suited for the determination of a continuous SQI. Another optimization process is therefore not pursued. By observing the SQI with respect to the absolute pulse error, an exponential correlation can be presumed. Therefore, the moving standard deviation of the standard error is calculated using a bootstrapping method. The averaged values of the standard deviations per window interval are then fitted using an exponential function. This is used for pulse rate correction, with respect to a fixed pulse rate error threshold. The estimated standard deviation is used to set this threshold.

3 Results

For the binary classification based on hand-annotated pulses the polynomial model with an order of five showed the best results. This leads to a sensitivity of 86 ± 15 % and a specificity of 94 ± 13 % for the dataset of the finger-PPG. The results of the inear-PPG fall slightly below the finger-PPG with a sensitivity of 77 ± 15 % and a specificity of 76 ± 20 %. By removing the negative classified pulses in the finger-PPG the pulse error rate can be improved from 1.24 ± 7.87 BPM to 0.71 ± 5.49 BPM. The same holds true for the inear-PPG, with an improvement from 3.56 ± 16.41 BPM to 2.93 ± 15.46 BPM.

For the binary classification based on a variable pulse rate error threshold, the feature-based model using a combination of the first derivative, the pulse length and the skewness, performs the best. A fixed threshold for error bounds is found. The classification results for both measurements are shown in figure 4. Thereby pulse rate errors in the finger-PPG greater than 5 BPM can be detected with a sensitivity of 91 ± 13 % and a specificity of 91 ± 15 %. Pulse rate errors less than 4 BPM are almost undetectable. The data set of the inear-PPG results in slightly better classification rates with a sensitivity of 91 ± 5 % and a specificity of 93 ± 16 % for pulse error rates above 6 BPM. In the last evaluation, which is based on

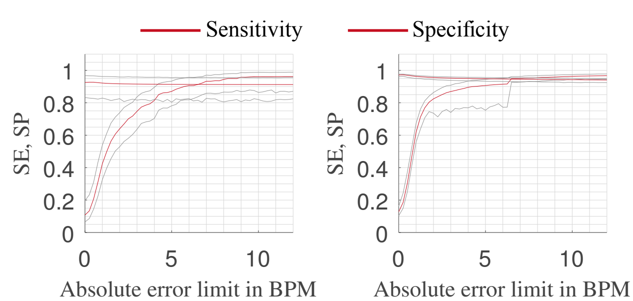

(a) Finger-PPG **(b)** Inear-PPG

Fig. 4: Sensitivity SE and specificity SP of the classification, calculated over all error borders using a fixed threshold. The classification result of the finger PPG and the inner ear PPG is shown in red. In grey the respective 95 % confidence intervals.

a continuous SQI, a direct functional correlation between the SQI and the standard deviation of the pulse rate error is shown. By using the moving standard deviation with a window size of 10 %, the bootstrap method reaches a 95 % confidence interval of ± 1.91 BPM. The exponential fitting takes place with a quadratic mean deviation of 0.94 BPM with an adjusted coefficient of determination of 0.94. The estimated standard deviation $\hat{\sigma}$ is shown in figure 5. The SQI thus shows a direct correlation with the standard deviation of the pulse rate error.

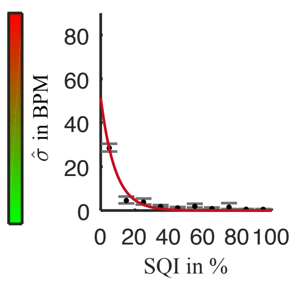

(a) Finger-PPG

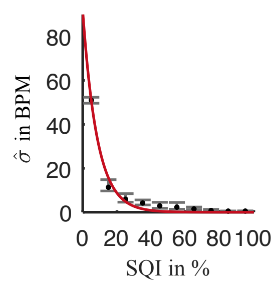

(b) Inear-PPG

Fig. 5: Curve fitting of the MD in χ^2-space with respect to the standard deviation.

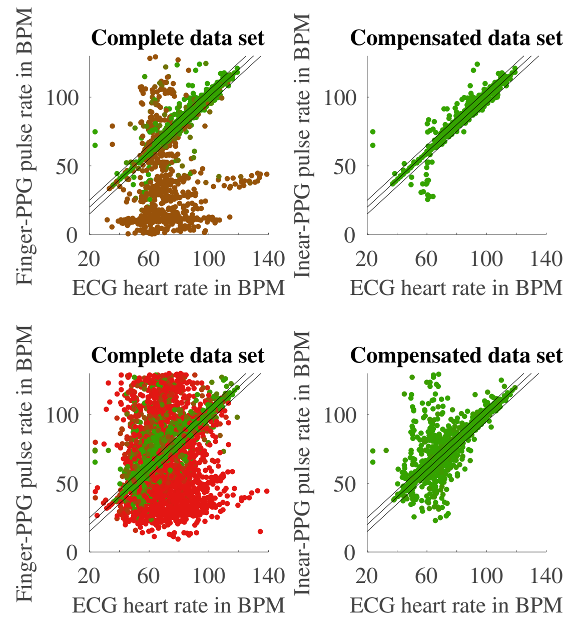

Fig. 6: Correction of the heart rate detection based on the pulse error barrier. Marked in black, the error bound $\mathcal{E} = 5$ BPM. The color mapping is based on the estimated standard deviation in figure 5.

This can be used for a correction of the pulse rate estimation, based on a variable error bound. In figure 6, a correction of pulse rate errors less then 5 BPM is done. This leads to a reduction of the pulse rate estimation error from 1.24 ± 7.87 BPM to 0.44 ± 1.39 BPM for the finger-PPG and 3.56 ± 16.41 BPM to 0.46 ± 2.09 BPM for the inear-PPG.

4 Conclusion & Outlook

The presented algorithm enables a robust detection of signal artifacts in PPG-signals with very good results. Compared to other algorithms, the novel algorithm shows particularly good classification results. The SQI can improve autonomous PPG analysis without ECG. Especially in the area of pulse rate variability analysis it can be a great benefit to have a signal quality information. Additionally, it can be used for battery saving methods in the area of mobile monitoring.

References

[1] Mohamed Elgendi. Optimal signal quality index for photoplethysmogram signals. *Bioengineering*, 3(4), 2016.

[2] Jyh-Jong Wei, Chuang-Jan Chang, Nai-Kuan Chou, and Gwo-Jen Jan. Ecg data compression using truncated singular value decomposition. *IEEE Transactions on Information Technology in Biomedicine*, 5(4):290–299, Dec 2001.

[3] Philippe Pierre Pebay. Formulas for robust, one-pass parallel computation of covariances and arbitrary-order statistical moments. Technical report, Sandia National Laboratories, 9 2008.

[4] Maik Pflugradt, Benjamin Moeller, and Reinhold Orglmeister. OPRA: A fast on-line signal quality estimator for pulsatile signals. *IFAC-PapersOnLine*, 48(20):459–464, 2015.

[5] Allan B Shang, Raymond T Kozikowski, Andrew W Winslow, and Sandy Weininger. Development of a standardized method for motion testing in pulse oximeters. *Anesthesia & Analgesia*, 105(6):S66–S77, 2007.

[6] T. Tigges, L. Bajrami, A. Pielmus, M. Klum, R. Orglmeister, L. Wiegand, and A. Feldheiser. Heart rate variability analysis during lower body negative pressure test induced central hypovolemia. *Current Directions in Biomedical Engineering*, 5:65–68, 09 2019.

[7] T. Tigges, A. Feldheiser, A. Pielmuş, M. Klum, L. Wiegank, and R. Orglmeister. Evaluation of pulse arrival times during lower body negative pressure test for the non-invasive detection of hypovolemia. In *2019 41st Annual International Conference of the IEEE Engineering in Medicine and Biology Society (EMBC)*, pages 3770–3774, 2019.

[8] B. P. Welford. Note on a method for calculating corrected sums of squares and products. *Technometrics*, 4(3):419–420, 1962.

[9] W. Zong, T. Heldt, GB. Moody, and RG. Mark. An open-source algorithm to detect onset of arterial blood pressure pulses. In *Computers in Cardiology, 2003*, pages 259–262. IEEE, 2003.